

## Integration of health monitoring and vibration control for smart building structures with time-varying structural parameters and unknown excitations

Y.L. Xu<sup>1</sup>, Q. Huang<sup>\*1,2</sup>, Y. Xia<sup>1</sup> and H.J. Liu<sup>2</sup>

<sup>1</sup>Department of Civil and Environmental Engineering, The Hong Kong Polytechnic University, Hong Kong  
<sup>2</sup>Shenzhen Graduate School, Harbin Institute of Technology, Shenzhen, China

(Received November 28, 2014, Revised January 19, 2015, Accepted January 21, 2015)

**Abstract.** When a building structure requires both health monitoring system and vibration control system, integrating the two systems together will be cost-effective and beneficial for creating a smart building structure with its own sensors (nervous system), processors (brain system), and actuators (muscular system). This paper presents a real-time integrated procedure to demonstrate how health monitoring and vibration control can be integrated in real time to accurately identify time-varying structural parameters and unknown excitations on one hand, and to optimally mitigate excessive vibration of the building structure on the other hand. The basic equations for the identification of time-varying structural parameters and unknown excitations of a semi-active damper-controlled building structure are first presented. The basic equations for semi-active vibration control of the building structure with time-varying structural parameters and unknown excitations are then put forward. The numerical algorithm is finally followed to show how the identification and the control can be performed simultaneously. The results from the numerical investigation of an example building demonstrate that the proposed method is feasible and accurate.

**Keywords:** building structure; identification; time-varying parameters; unknown excitation; vibration control; semi-active dampers; integration; smart building

---

### 1. Introduction

In the last few decades, a great deal of research has been conducted on health monitoring and vibration control of building structures subject to earthquakes, strong winds, and other natural or man-made hazards. Comprehensive reviews on vibration control technologies for civil structures were given by Housner *et al.* (1997), Nishitani and Inoue (2001), and Spencer *et al.* (2003). There are also many state-of-the-art reports on health monitoring technologies for civil structures (e.g., Doebling *et al.* 1996, Mufti 2001, Sohn *et al.* 2003, Wenzel 2009, Xu and Xia 2012). However, the areas of vibration control and health monitoring have mostly been investigated separately although both vibration control system and health monitoring system need similar sensors, data acquisition, transmission and processing devices. When a building structure requires both vibration control system and health monitoring system, integrating both systems together will be cost-effective by

---

\*Corresponding author, Ph.D., Research Assistant, E-mail: [tmxhq@126.com](mailto:tmxhq@126.com)

sharing the same hardware devices and beneficial for creating a smart structure with its own sensors (nervous system), processor (brain system), and actuators (muscular system).

In mechanical engineering, Ray and Tian (1999) introduced a method of enhancing modal frequency sensitivity to damage using a feedback control that intended for smart structures embodying self-actuation and self-sensing capabilities. Gattulli and Romeo (2000) presented an integrated procedure based on a direct adaptive control algorithm for uncertain multi-degree-of-freedom (MDOF) systems. Viscardi and Lecce (2002) proposed an integrated system for active vibro-acoustic control and damage detection on a typical aeronautical structure based on piezoelectric devices. Deng *et al.* (2011) proposed a self-adaptive modal control including both identification and control update in real-time. However, these studies focused on actively controlled mechanical systems that are different from civil structures where structural systems are more complicated with uncertainties and active control may become problematic.

In civil engineering, Nagarajaiah and Jung (2014) reviewed a number of recent papers on vibration frequency tracking and semi-active control of building structures using smart tuned mass dampers. Xu and Chen (2008), Chen and Xu (2008), and Chen *et al.* (2010) proposed an integrated procedure of vibration control and health monitoring of building structures in the frequency-domain and the time-domain respectively, using semi-active friction dampers to fulfill model updating, seismic response control and damage detection of the building structure based on the change of natural frequencies and mode shapes. Huang *et al.* (2012) and Xu *et al.* (2014) extended their methods in the frequency domain based on the change of frequency response functions. Nevertheless, these procedures cannot realize real-time integration of vibration control and health monitoring of building structures. Recently, Yang *et al.* (2013) presented a hybrid real-time structural health monitoring and control system for building structures, in which a model-reference adaptive control algorithm was integrated with an inter-story drift-based acceleration feedback method for health monitoring. In their study, the earthquake-induced ground excitation to a building structure was assumed to be known for both vibration control and health monitoring, and structural vibration control was implemented using active control technology.

For civil structures, external excitations such as earthquake-induced ground motion and typhoon-induced buffeting forces are difficult, if not impossible, to be measured directly and accurately on site. The real-time identification of external excitation for both vibration control and health monitoring is necessary. Moreover, even for a building structure with control devices, structural damage may occur during an extreme event and structural parameters of damaged components are actually varying with time. To ensure control performance, time-varying structural parameters shall be identified and control parameters shall be adjusted accordingly. It shall be noted that the identification of time-varying structural parameters in such a case is for a controlled building structure and thus real-time control forces shall be taken into consideration in the identification.

This paper presents a real-time integrated procedure to demonstrate how health monitoring and vibration control can be integrated in real time to accurately identify time-varying structural parameters and unknown excitations on one hand, and to optimally mitigate excessive vibration of the building structure on the other hand. The basic equations for the identification of time-varying structural parameters and unknown excitations of a magneto-rheological (MR) damper-controlled building structure under earthquake excitation are first presented based on the least-squares estimation method as well as the measured structural responses and control forces. The basic equations for semi-active control of the building structure with MR dampers and clipped optimal displacement control algorithm are put forward based on the updated time-varying structural

parameters and unknown excitations. The numerical algorithm is then followed to perform both identification and control simultaneously. The feasibility and accuracy of the proposed method is finally examined through the numerical investigation of an example building.

## 2. Structural health monitoring

For a building structure subject to earthquake-induced ground excitation (see Fig. 1), damage may occur and the structural parameters of damaging structural components may vary with time during the ground excitation. To detect damage and identify time-varying structural parameters on-line in the time domain, a structural health monitoring system including sensors, data transmission system, data acquisition system and data analysis system should be installed in the building structure to provide essential and correct information. If the earthquake-induced ground excitation cannot be directly measured, the identification of ground excitation is also necessary. In some cases, the building structure is equipped with control devices to mitigate seismic-induced vibration. Therefore, the identification of time-varying structural parameters and ground excitation of a controlled building structure is an important part of structural health monitoring. In this section, the basic equations for the identification of time-varying structural parameters and unknown excitations of a MR damper-controlled building structure under earthquake excitation are presented based on the least-squares estimation method as well as the measured structural responses and control forces. Although the identification of time-varying structural parameters and unknown excitation was investigated before using the wavelet analysis (Basu *et al.* 2008), neural estimation method (Kosmatopoulos *et al.* 2001), least-squares estimation method (Yang and Huang 2007, Yang *et al.* 2007), and the extended Kalman filter method (Lei *et al.* 2012a, Lei *et al.* 2012b), the method proposed in this study is more accurate and efficient.

### 2.1 Equation of motion

In this study, the structural mass matrix  $\mathbf{M}$  is assumed to be known and constant for the simplicity of presentation although it is not absolutely necessary. Other structural parameters, such as damping and stiffness coefficients, are time-varying as structural damage occurs with time. Excitations on a controlled building structure can be separated into two parts: control forces and unknown excitations. Consequently, the second-order differential equation of motion of a building structure with  $n$  degrees-of-freedom (DOF) is given by

$$\mathbf{M}\ddot{\mathbf{X}}(t) + \mathbf{C}(t)\dot{\mathbf{X}}(t) + \mathbf{K}(t)\mathbf{X}(t) = \boldsymbol{\phi}^*\mathbf{f}^*(t) + \boldsymbol{\phi}\mathbf{f}(t) \quad (1)$$

where  $\mathbf{M}$ ,  $\mathbf{C}(t)$  and  $\mathbf{K}(t)$  represent the  $n \times n$  mass, damping and stiffness matrices of the building structure, respectively;  $\ddot{\mathbf{X}}(t)$ ,  $\dot{\mathbf{X}}(t)$  and  $\mathbf{X}(t)$  are the  $n \times 1$  structural acceleration, velocity and displacement response vectors, respectively;  $\mathbf{f}^*(t)$  is the  $r \times 1$  measured control force vector with the influence matrix  $\boldsymbol{\phi}^*$  ( $n \times r$ ); and  $\mathbf{f}(t)$  is the  $s \times 1$  unknown excitation vector with the influence matrix  $\boldsymbol{\phi}$  ( $n \times s$ ).

For the controlled building structure with semi-active MR dampers and subjected to earthquake excitation, the semi-active control forces could be measured by force transducers to form the measured control force vector, while the earthquake-induced ground acceleration could be treated

as the unknown excitation vector.

## 2.2 Multiple linear regression equation

Suppose that  $\mathbf{Z}$  is an  $m \times 1$  unknown time-varying structural parameter vector, which can include both structural stiffness and damping parameters. The unknown time-varying structural parameter vector at time  $t = k\Delta t$  is denoted as  $\mathbf{Z}_k$ , in which  $\Delta t$  is the sampling interval.

The observation (measurement) equation associated with Eq. (1) at time  $t = k\Delta t$  can be described as

$$\mathbf{y}_k = \mathbf{H}_k \mathbf{Z}_k - \boldsymbol{\phi} \mathbf{f}_k + \mathbf{v}_k \quad (2)$$

where  $\mathbf{y}_k = -\mathbf{M}\ddot{\mathbf{X}}_k + \boldsymbol{\phi}^* \mathbf{f}_k^*$  is a  $n \times 1$  measurement vector which can be obtained by the measured structural acceleration responses  $\ddot{\mathbf{X}}_k$  and the measured control forces  $\mathbf{f}_k^*$ ;  $\mathbf{H}_k$  is an  $n \times m$  observation matrix composed of the measured structural velocity and displacement responses  $\dot{\mathbf{X}}_k$  and  $\mathbf{X}_k$ ;  $\mathbf{v}_k$  represents a  $n \times 1$  noise vector, taking into consideration the model uncertainty of the structure and the measurement noise. The subscript  $k$  represents the values of matrices or vectors at time  $t = k\Delta t$ .

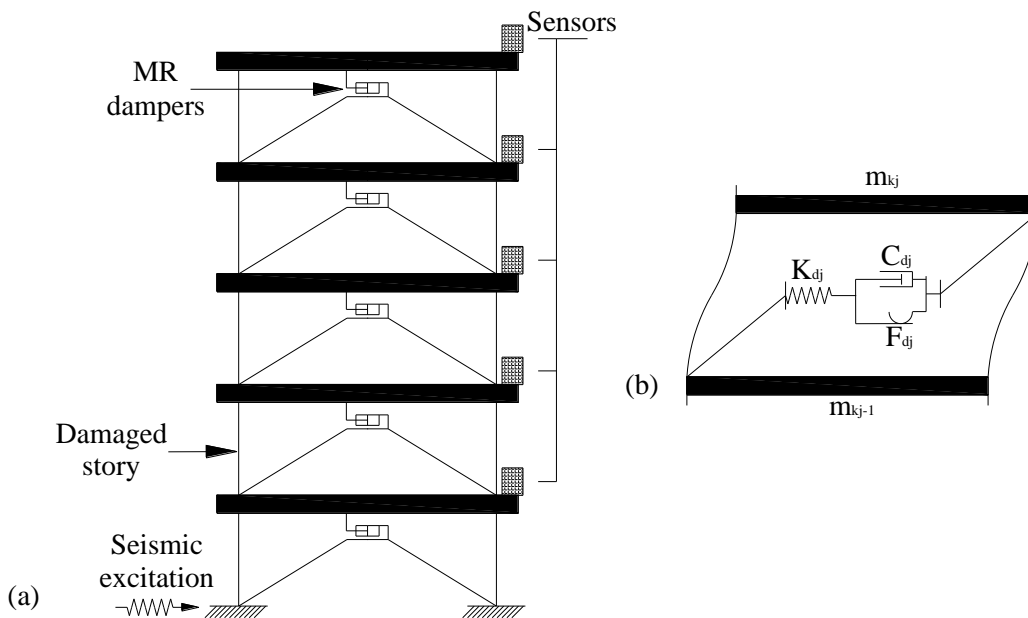


Fig. 1 Schematic diagram of a building structure with integrated health monitoring and vibration control system. (a) sensors and MR dampers and (b) mechanical model of MR damper-brace system

There are two variable vectors  $\mathbf{Z}_k$  and  $\mathbf{f}_k$  in Eq. (2) to be predicted. Therefore, Eq. (2) is a multiple linear regression equation. Furthermore, the elements in the predictor variable vectors are time-varying. The traditional least-squares estimation method for solving the simple linear regression equation to find constant structural parameters cannot be directly applied to Eq. (2).

### 2.3 Transformation to simple linear regression equation

From Eq. (2), one can obtain

$$\boldsymbol{\Phi}\mathbf{f}_k = -\mathbf{y}_k + \mathbf{H}_k\mathbf{Z}_k + \mathbf{v}_k \tag{3}$$

The closest solution of  $\mathbf{f}_k$  in Eq. (3) can be given by the following projection matrix.

$$\mathbf{f}_{k,LS} = (\boldsymbol{\Phi}^T\boldsymbol{\Phi})^{-1}\boldsymbol{\Phi}^T(-\mathbf{y}_k + \mathbf{H}_k\mathbf{Z}_k + \mathbf{v}_k) \tag{4}$$

The error of the solution from Eq. (4) is given by

$$\begin{aligned} err &= \boldsymbol{\Phi}\mathbf{f}_k - \boldsymbol{\Phi}\mathbf{f}_{k,LS} \\ &= (-\mathbf{y}_k + \mathbf{H}_k\mathbf{Z}_k + \mathbf{v}_k) - \boldsymbol{\Phi}(\boldsymbol{\Phi}^T\boldsymbol{\Phi})^{-1}\boldsymbol{\Phi}^T(-\mathbf{y}_k + \mathbf{H}_k\mathbf{Z}_k + \mathbf{v}_k) \\ &= (\mathbf{I}_n - \boldsymbol{\Phi}(\boldsymbol{\Phi}^T\boldsymbol{\Phi})^{-1}\boldsymbol{\Phi}^T)(-\mathbf{y}_k + \mathbf{H}_k\mathbf{Z}_k + \mathbf{v}_k) \end{aligned} \tag{5}$$

in which  $\mathbf{I}_n$  is the  $n \times n$  identity matrix; and the matrix  $\boldsymbol{\Phi}(\boldsymbol{\Phi}^T\boldsymbol{\Phi})^{-1}\boldsymbol{\Phi}^T$  is the projection matrix that projects the vector  $-\mathbf{y}_k + \mathbf{H}_k\mathbf{Z}_k + \mathbf{v}_k$  on to the space spanned by the columns of  $\boldsymbol{\Phi}$ . As a limit, the error in Eq. (5) tends to be zero, leading to

$$\boldsymbol{\Phi}\mathbf{y}_k = \boldsymbol{\Phi}\mathbf{H}_k\mathbf{Z}_k + \boldsymbol{\Phi}\mathbf{v}_k \tag{6}$$

where  $\boldsymbol{\Phi} = \mathbf{I}_n - \boldsymbol{\Phi}(\boldsymbol{\Phi}^T\boldsymbol{\Phi})^{-1}\boldsymbol{\Phi}^T$  for the simplicity of presentation. It is noted that the projection matrix and naturally the matrix  $\boldsymbol{\Phi}$  has the two properties: (1)  $\boldsymbol{\Phi}$  is a symmetric matrix,  $\boldsymbol{\Phi}^T = \boldsymbol{\Phi}$ ; and (2)  $\boldsymbol{\Phi}^2 = \boldsymbol{\Phi}$ . As a result, the multiple linear regression equation expressed by Eq. (2) is transformed into the simple linear regression equation expressed by Eq. (6).

### 2.4 Recursive least-squares estimation for time-varying parameters

When a structure is being damaged, the structural parameters vary with time. To track the parametric variation due to damage with unknown inputs, Yang *et al.* (2007) implemented the adaptive tracking technique into their recursive least-squares estimation with unknown inputs (ARLSE-UI). In this study, a simple time-varying correction factor is introduced together with Eq. (6) to identify the parametric variations due to structural damage. The recursive least squares estimation of Eq. (6) yields

$$\hat{\mathbf{Z}}_k = \hat{\mathbf{Z}}_{k-1} + \mathbf{K}_k(\boldsymbol{\Phi}\mathbf{y}_k - \boldsymbol{\Phi}\mathbf{H}_k\hat{\mathbf{Z}}_{k-1}) = \hat{\mathbf{Z}}_{k-1} + \mathbf{K}_k\boldsymbol{\Phi}(\mathbf{y}_k - \mathbf{H}_k\hat{\mathbf{Z}}_{k-1}) \tag{7}$$

where  $\hat{\mathbf{Z}}_k$  and  $\hat{\mathbf{Z}}_{k-1}$  are the estimated values of  $\mathbf{Z}$  at time  $t=k\Delta t$  and  $t=(k-1)\Delta t$  respectively;  $\mathbf{K}_k$  is the least-squares estimation (LSE) gain matrix for  $\hat{\mathbf{Z}}_k$  at time  $t=k\Delta t$  with a size of  $m \times n$ ; and the term  $\Phi \mathbf{y}_k - \Phi \mathbf{H}_k \hat{\mathbf{Z}}_{k-1}$  is the correction term.

The current estimation error  $\boldsymbol{\varepsilon}_k$  of the unknown parameter vector  $\mathbf{Z}_k$  at time  $t=k\Delta t$  can be obtained as follows

$$\begin{aligned} \boldsymbol{\varepsilon}_k &= \mathbf{Z}_k - \hat{\mathbf{Z}}_k \\ &= \mathbf{Z}_k - \hat{\mathbf{Z}}_{k-1} - \mathbf{K}_k (\Phi \mathbf{y}_k - \Phi \mathbf{H}_k \hat{\mathbf{Z}}_{k-1}) \\ &= \mathbf{Z}_k - \hat{\mathbf{Z}}_{k-1} - \mathbf{K}_k (\Phi \mathbf{H}_k \mathbf{Z}_k + \Phi \mathbf{v}_k - \Phi \mathbf{H}_k \hat{\mathbf{Z}}_{k-1}) \\ &= (\mathbf{I}_m - \mathbf{K}_k \Phi \mathbf{H}_k) (\mathbf{Z}_k - \hat{\mathbf{Z}}_{k-1}) - \mathbf{K}_k \Phi \mathbf{v}_k \end{aligned} \quad (8)$$

in which  $\mathbf{I}_m$  is the  $m \times m$  identity matrix. If the structural parameters are constants, i.e.,  $\mathbf{Z}_k = \mathbf{Z}_{k-1}$ , one can then have  $\mathbf{Z}_k - \hat{\mathbf{Z}}_{k-1} = \mathbf{Z}_{k-1} - \hat{\mathbf{Z}}_{k-1} = \boldsymbol{\varepsilon}_{k-1}$ . However, the structural parameters vary with time such as a degradation of stiffness when structural damage occurs. To track the structural parametric variations and consequently detect structural damage on-line, a time-varying correction factor matrix  $\boldsymbol{\lambda}_k$  is introduced to reflect the structural parametric variations as follows

$$\mathbf{Z}_k - \hat{\mathbf{Z}}_{k-1} = \boldsymbol{\lambda}_k (\mathbf{Z}_{k-1} - \hat{\mathbf{Z}}_{k-1}) = \boldsymbol{\lambda}_k \boldsymbol{\varepsilon}_{k-1} \quad (9)$$

in which  $\boldsymbol{\lambda}_k$  is a diagonal matrix with size of  $m \times m$ . By substituting Eq. (9) into Eq.(8), the current estimation error  $\boldsymbol{\varepsilon}_k$  could be calculated by

$$\boldsymbol{\varepsilon}_k = (\mathbf{I}_m - \mathbf{K}_k \Phi \mathbf{H}_k) \boldsymbol{\lambda}_k \boldsymbol{\varepsilon}_{k-1} - \mathbf{K}_k \Phi \mathbf{v}_k \quad (10)$$

It is noted that  $\Phi$  is a symmetric matrix. The estimation error covariance can be obtained as

$$\begin{aligned} \mathbf{P}_k &= \mathbf{E}(\boldsymbol{\varepsilon}_k \boldsymbol{\varepsilon}_k^T) \\ &= \mathbf{E}\{[(\mathbf{I}_m - \mathbf{K}_k \Phi \mathbf{H}_k) \boldsymbol{\lambda}_k \boldsymbol{\varepsilon}_{k-1} - \mathbf{K}_k \Phi \mathbf{v}_k][(\mathbf{I}_m - \mathbf{K}_k \Phi \mathbf{H}_k) \boldsymbol{\lambda}_k \boldsymbol{\varepsilon}_{k-1} - \mathbf{K}_k \Phi \mathbf{v}_k]^T\} \\ &= (\mathbf{I}_m - \mathbf{K}_k \Phi \mathbf{H}_k) \boldsymbol{\lambda}_k \mathbf{E}(\boldsymbol{\varepsilon}_{k-1} \boldsymbol{\varepsilon}_{k-1}^T) \boldsymbol{\lambda}_k^T (\mathbf{I}_m - \mathbf{K}_k \Phi \mathbf{H}_k)^T - \mathbf{K}_k \Phi \mathbf{E}(\mathbf{v}_k \boldsymbol{\varepsilon}_{k-1}^T) \boldsymbol{\lambda}_k^T (\mathbf{I}_m - \mathbf{K}_k \Phi \mathbf{H}_k)^T \\ &\quad - (\mathbf{I}_m - \mathbf{K}_k \Phi \mathbf{H}_k) \boldsymbol{\lambda}_k \mathbf{E}(\boldsymbol{\varepsilon}_{k-1} \mathbf{v}_k^T) (\mathbf{K}_k \Phi)^T + \mathbf{K}_k \Phi \mathbf{E}(\mathbf{v}_k \mathbf{v}_k^T) (\mathbf{K}_k \Phi)^T \\ &= (\mathbf{I}_m - \mathbf{K}_k \Phi \mathbf{H}_k) \boldsymbol{\lambda}_k \mathbf{P}_{k-1} \boldsymbol{\lambda}_k^T (\mathbf{I}_m - \mathbf{K}_k \Phi \mathbf{H}_k)^T + \mathbf{K}_k \Phi \mathbf{R}_k \Phi \mathbf{K}_k^T \end{aligned} \quad (11)$$

where  $\mathbf{R}_k = \mathbf{E}(\mathbf{v}_k \mathbf{v}_k^T)$  is the covariance of noise  $\mathbf{v}_k$ . Moreover, the estimation error  $\boldsymbol{\varepsilon}_{k-1}$  at time  $t=(k-1)\Delta t$  can be assumed to be independent of the noise vector  $\mathbf{v}_k$  at time  $t=k\Delta t$ , and accordingly  $\mathbf{E}(\mathbf{v}_k \boldsymbol{\varepsilon}_{k-1}^T) = \mathbf{E}(\boldsymbol{\varepsilon}_{k-1} \mathbf{v}_k^T) = \mathbf{0}$  in Eq. (11).

The time-varying correction factor matrix  $\lambda_k$  can be calculated based on the current measurements. It is noted from Eq. (7) that the current correction term at time  $t = k\Delta t$  can be calculated based on the current measurements as follows

$$\mathbf{r}_k = \Phi \mathbf{y}_k - \Phi \mathbf{H}_k \hat{\mathbf{Z}}_{k-1} = \Phi \mathbf{H}_k (\mathbf{Z}_k - \hat{\mathbf{Z}}_{k-1}) + \Phi \mathbf{v}_k = \Phi \mathbf{H}_k \lambda_k \boldsymbol{\varepsilon}_{k-1} + \Phi \mathbf{v}_k \quad (12)$$

Hence, the time-varying factor correction matrix  $\lambda_k$  can be determined by the following equation

$$\mathbf{P}_{r,k} = E(\mathbf{r}_k \mathbf{r}_k^T) = \Phi \mathbf{H}_k \lambda_k \mathbf{P}_{k-1} \lambda_k^T \mathbf{H}_k^T \Phi + \Phi \mathbf{R}_k \Phi \quad (13)$$

To obtain the optimal value of the gain matrix  $\mathbf{K}_k$  that can minimize the estimation error covariance  $\mathbf{P}_k$  at time  $t = k\Delta t$ , the differentiation of  $\mathbf{P}_k$  in Eq. (11) with respect to  $\mathbf{K}_k$  produces

$$\begin{aligned} \partial \mathbf{P}_k / \partial \mathbf{K}_k &= 2(\mathbf{I}_m - \mathbf{K}_k \Phi \mathbf{H}_k) \lambda_k \mathbf{P}_{k-1} \lambda_k^T (-\Phi \mathbf{H}_k)^T + 2\mathbf{K}_k \Phi \mathbf{R}_k \Phi \\ &= 2\mathbf{K}_k \Phi (\mathbf{H}_k \lambda_k \mathbf{P}_{k-1} \lambda_k^T \mathbf{H}_k^T + \mathbf{R}_k) \Phi - 2\lambda_k \mathbf{P}_{k-1} \lambda_k^T \mathbf{H}_k^T \Phi \end{aligned} \quad (14)$$

By setting the value of the partial derivative to zero, one can obtain

$$\mathbf{K}_k = \lambda_k \mathbf{P}_{k-1} \lambda_k^T \mathbf{H}_k^T \Phi / [\Phi (\mathbf{H}_k \lambda_k \mathbf{P}_{k-1} \lambda_k^T \mathbf{H}_k^T + \mathbf{R}_k) \Phi] \quad (15)$$

It is noted that  $\mathbf{P}_{k-1}$ ,  $\mathbf{R}_k$  and  $\Phi$  are symmetric matrices, the estimation error covariance expressed by Eq. (11) could be simplified in terms of Eq. (15) as

$$\begin{aligned} \mathbf{P}_k &= (\mathbf{I}_m - \mathbf{K}_k \Phi \mathbf{H}_k) \lambda_k \mathbf{P}_{k-1} \lambda_k^T (\mathbf{I}_m - \mathbf{K}_k \Phi \mathbf{H}_k)^T + \mathbf{K}_k \Phi \mathbf{R}_k \Phi \mathbf{K}_k^T \\ &= (\mathbf{I}_m - \mathbf{K}_k \Phi \mathbf{H}_k) \lambda_k \mathbf{P}_{k-1} \lambda_k^T - \lambda_k \mathbf{P}_{k-1} \lambda_k^T \mathbf{H}_k^T \Phi \mathbf{K}_k^T + \mathbf{K}_k \Phi (\mathbf{H}_k \lambda_k \mathbf{P}_{k-1} \lambda_k^T \mathbf{H}_k^T + \mathbf{R}_k) \Phi \mathbf{K}_k^T \\ &= (\mathbf{I}_m - \mathbf{K}_k \Phi \mathbf{H}_k) \lambda_k \mathbf{P}_{k-1} \lambda_k^T \end{aligned} \quad (16)$$

Once the estimate value  $\hat{\mathbf{Z}}_k$  of the unknown parametric vector at time  $t = k\Delta t$  is calculated by Eq. (7), the estimate value of the unknown excitation vector at time  $t = k\Delta t$  can be estimated by

$$\hat{\mathbf{f}}_k = -(\Phi^T \Phi)^{-1} \Phi^T (\mathbf{y}_k - \mathbf{H}_k \hat{\mathbf{Z}}_k) \quad (17)$$

Eqs. (7), (13), (15) (16) and (17) form the recursive least-squares estimation for identifying both time-varying structural parameters and unknown excitations. If all the external excitations can be measured and the unknown parametric vector is constant (the influence matrix of the unknown excitation vector  $\Phi$  in Eq. (1) is a null matrix leading to  $\Phi = \mathbf{I}_n$  and the time-varying correction factor matrix  $\lambda_k = \mathbf{I}_m$ ), the proposed algorithm becomes the same as the traditional recursive least-squares estimation method.

The proposed algorithm can identify the unknown inputs and time-varying structural parameters simultaneously, and the flow chart of the proposed recursive least-squares estimation algorithm is shown in Fig. 2.

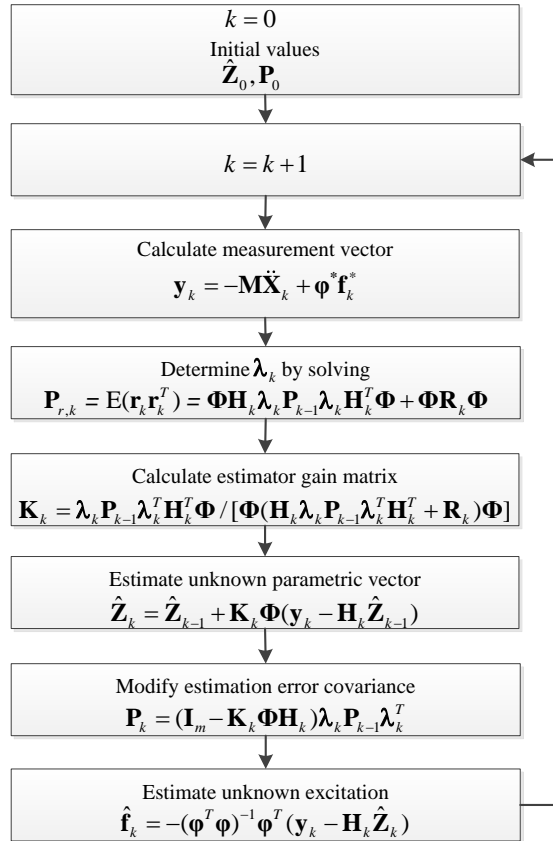


Fig. 2 Flowchart of the proposed method for identifying time-varying structural parameters and unknown excitations

### 3. Structural vibration control

When a building structure is subject to earthquake excitation, excessive vibration may occur and cause damage (see Fig. 1). Semi-active dampers can be installed in the building structure to reduce the excessive vibration and damage. The vibration control system, including sensors, semi-active dampers, data transmission system, data acquisition system, control algorithm, and data analysis system, should be installed in the building structure to provide essential feedback information and form a close loop control. The semi-active vibration control is then implemented based on the measured structural responses and the identified time-varying structural parameters to generate optimal control forces and achieve the maximum building response reduction. In this section, the basic equations for semi-active control of the building structure with MR dampers and clipped optimal displacement control algorithm are put forward based on the updated time-varying structural parameters and unknown excitations.

### 3.1 Mechanical model of a MR damper

There are a number of mechanical models available to describe the relationship between force and motion of a MR damper. For the sake of simplicity to illustrate the integration of structural control and health monitoring in this study, the simple Bingham model is adopted. For a steady and fully developed flow, the Bingham model can be used for the shear resistance of MR fluids, which has a friction component augmented by a Newtonian viscosity component. The relationship between the force  $P_d$  and velocity  $\dot{e}$  of the MR damper can be expressed as follows (Gavin *et al.* 1996, Xu *et al.* 2000, Qu and Xu 2001)

$$P_d(t) = C_d \dot{e} + F_d \operatorname{sgn}(\dot{e}) \quad (18)$$

in which

$$C_d = C_1 \frac{12\zeta LA_p}{bh^3} A_p, \quad F_d = C_2 \frac{L\tau_y}{h} A_p + P_y \quad (19)$$

For the flow-type damper

$$C_1 = 1.0, \quad C_2 = 2.07 + \frac{1.0}{1.0 + 0.4T}, \quad T = \frac{bh^2\tau_y}{12A_p\zeta\dot{e}} \quad (20)$$

For the mixed-type damper

$$C_1 = 1.0 - \frac{bh}{2A_p}, \quad C_2 = 2.07 + \frac{1.0}{1.0 + 0.4T} - \frac{1.5V_2}{1.0 + 0.4T^2}, \quad V = \frac{bh}{2A_p} \quad (21)$$

where  $b$  is the width of the rectangular plate;  $h$  is the gap between two parallel plates;  $L$  is the effective axial pole length;  $A_p$  is the cross-sectional area of the piston;  $\tau_y$  represents the yielding shear stress controlled by the applied field; and  $P_y$  is the mechanical friction force in the damper.

Clearly,  $F_d$  is the function of yielding shear stress and it can be controlled through the applied field but  $C_d$  is independent of the applied field.

Let us consider a multi-story shear building subjected to earthquake excitation as shown in Fig. 1(a), semi-active MR dampers can be positioned between the chevron braces and the rigid floor diaphragms to enhance its vibration energy dissipation capacity. In consideration of the stiffness of chevron brace, the mechanical model for the MR damper-chevron brace system can be seen as a damper and a spring being connected in series as shown in Fig. 1(b). When considering the MR damper and the chevron brace to be connected in series, the spring force in the brace is equal to the force on the piston of the damper. Eq. (18) should thus be correspondingly changed to

$$C_d \dot{e} + F_d \operatorname{sgn}(\dot{e}) = K_d (u - e) \quad (22)$$

where  $u$  is the relative displacement between the two floors with the damper installed and  $K_d$  is the horizontal stiffness of the chevron brace.

### 3.2 Equation of motion

In terms of Eq. (22), the equation of motion of an  $n$ -story frame structure with  $m$  dampers subject to earthquake excitation can be expressed as

$$\mathbf{M}\ddot{\mathbf{X}}(t) + \mathbf{C}(t)\dot{\mathbf{X}}(t) + (\mathbf{K}(t) + \mathbf{H}_c\mathbf{K}_d\mathbf{H}_c^T)\mathbf{X}(t) + \mathbf{H}_c\mathbf{K}_d\mathbf{e}(t) = \mathbf{H}_e\ddot{\mathbf{x}}_g(t) \quad (23)$$

$$\frac{C_{d_j}}{K_{d_j}}\dot{e}_j + e_j + \frac{F_{d_j}}{K_{d_j}}\text{sgn}(\dot{e}_j) = \mathbf{H}_{c_j}^T\mathbf{X} = X_{kj} - X_{kj-1} \quad (j = 1, 2, \dots, m) \quad (24)$$

where  $\mathbf{C}(t)$  and  $\mathbf{K}(t)$  are the  $n \times n$  mass, damping, and stiffness matrices of the frame structure, respectively, which are the same as those in Eq. (1);  $\mathbf{C}(t)$  and  $\mathbf{K}(t)$  are the time-varying structural damping and stiffness matrices which are updated by the health monitoring system with time;  $\mathbf{K}_d$  is the  $m \times m$  diagonal stiffness matrix, of which the element is the stiffness coefficient of the chevron brace;  $m$  is the number of stories with MR dampers installed;  $\mathbf{H}_c$  is the  $n \times m$  matrix converting the brace stiffness matrix into the global co-ordinate system; the superscript T means the transposition of a matrix;  $\mathbf{X}$ ,  $\dot{\mathbf{X}}$ , and  $\ddot{\mathbf{X}}$  are the  $n \times 1$  relative displacement, velocity, and acceleration vectors of the frame structure with respect to the ground, respectively;  $\mathbf{e}$  is the  $m \times 1$  displacement vector of the MR dampers;  $\mathbf{H}_{c_j}$  is the  $j$ th column vector of the matrix  $\mathbf{H}_c$ ;  $X_{kj}$  and  $X_{kj-1}$  are the displacements of the top and bottom floors of the  $k$ th story where the  $j$ th damper is installed.

Eq. (23) can be written to the same form as Eq. (1) by using the following substitutions.

$$\boldsymbol{\phi}^* = \mathbf{H}_c, \quad \mathbf{f}^*(t) = -\mathbf{K}_d[\mathbf{H}_c^T\mathbf{X}(t) + \mathbf{e}(t)], \quad \boldsymbol{\phi} = \mathbf{H}_e, \quad \mathbf{f}(t) = \ddot{\mathbf{x}}_g(t) \quad (25)$$

Eq. (23) can also be replaced by an equivalent first-order differential equation of the state-space form

$$\dot{\mathbf{Z}}_{MR}(t) = \mathbf{A}_{MR}(t)\mathbf{Z}_{MR}(t) + \mathbf{B}_{MR}\mathbf{e}(t) + \mathbf{D}_{MR}\ddot{\mathbf{x}}_g(t) \quad (26)$$

in which

$$\mathbf{A}_{MR}(t) = \begin{bmatrix} \mathbf{0} & \mathbf{I} \\ -\mathbf{M}^{-1}(\mathbf{K}(t) + \mathbf{H}_c\mathbf{K}_d\mathbf{H}_c^T) & -\mathbf{M}^{-1}\mathbf{C}(t) \end{bmatrix}, \quad \mathbf{B}_{MR} = \begin{bmatrix} \mathbf{0} \\ \mathbf{M}^{-1}\mathbf{H}_c\mathbf{K}_d \end{bmatrix}, \quad \mathbf{D}_{MR} = \begin{bmatrix} \mathbf{0} \\ \mathbf{M}^{-1}\mathbf{H}_e \end{bmatrix}, \quad \mathbf{Z}_{MR}(t) = \begin{bmatrix} \mathbf{X}(t) \\ \dot{\mathbf{X}}(t) \end{bmatrix} \quad (27)$$

In this study, the stiffness matrix and damping matrix of the building structure is constructed using the stiffness coefficients and damping coefficients that are identified from the health monitoring system in real time. Accordingly, the matrix  $\mathbf{A}_{MR}(t)$  in Eq. (27) is reconstructed at each time step of the computation.

### 3.3 Semi-active control algorithm

Xu *et al.* (2000) presented a clipped optimal displacement control approach in terms of the linear quadratic regular (LQR) control theory that minimizes

$$J = \int_0^{t_f} [\mathbf{Z}_{MR}^T(t)\mathbf{Q}_{MR}\mathbf{Z}_{MR}(t) + \mathbf{e}^T(t)\mathbf{R}_{MR}\mathbf{e}(t)]dt \tag{28}$$

to control the displacement vector  $\mathbf{e}_T(t)$  as

$$\mathbf{e}_T(t) = -\mathbf{R}_{MR}\mathbf{B}_{MR}\mathbf{P}_{MR}(t)\mathbf{Z}_{MR}(t) \tag{29}$$

where  $\mathbf{Q}_{MR}$  is the weighting matrix for the structure response in the optimal displacement control, it is an  $n \times n$  positive semi-definite matrix;  $\mathbf{R}_{MR}$  is the weighting matrix for the damper displacement in the optimal displacement control, it is an  $m \times m$  positive definite matrix; the two weighting matrices  $\mathbf{Q}_{MR}$  and  $\mathbf{R}_{MR}$  are often determined by trial and error for the concerned problem; and  $\mathbf{P}_{MR}(t)$  is the positive definite solution of the following Riccati equation

$$\mathbf{P}_{MR}(t)\mathbf{B}_{MR}^T\mathbf{R}_{MR}^{-1}\mathbf{B}_{MR}\mathbf{P}_{MR}(t) - \mathbf{A}_{MR}^T(t)\mathbf{P}_{MR}(t) - \mathbf{P}_{MR}(t)\mathbf{A}_{MR}(t) - \mathbf{Q}_{MR} = 0 \tag{30}$$

The strategy in the clipped optimal displacement control approach (Xu *et al.* 2000) can be described as follows. When the  $j$ th damper displacement  $e_j$  is approaching the desired optimal damper displacement vector  $e_{Tj}$ , the friction force  $F_{dj}$  in the damper is set to its minimum value. When the  $j$ th damper moves in the opposite direction to the optimal damper displacement, the friction force  $F_{dj}$  in the damper should be set to a smaller value of the two quantities:  $F_{\max}$  and the actual damper force  $K_{dj}(X_{kj} - X_{kj-1} - e_j)$  minus a small quantity  $F_0$ . In this way, the damper is always in motion to dissipate vibration energy. This strategy can be stated as

$$F_{dj} = \begin{cases} F_{\min} & \text{when } e_j(e_{Tj} - \dot{e}_j) > 0 \\ \min\{\text{abs}[K_{dj}(X_{kj} - X_{kj-1} - e_j)] - F_0, F_{\max}\} & \text{when } e_j(e_{Tj} - \dot{e}_j) < 0 \end{cases} \quad (j=1, 2, \dots, m) \tag{31}$$

The flow chart of the proposed semi-active control with MR dampers is shown in Fig. 3.

### 4. Integrated numerical algorithm

Based on the equations presented in the previous two sections, an integrated numerical algorithm can be implemented for real-time system identification and vibration control of the building structure step by step as follows:

Step 1: Obtain time-varying factor correction matrix  $\lambda_k$  at time  $t = k\Delta t$  by solving Eq. (13) based on the current measurements  $\mathbf{y}_k$ .

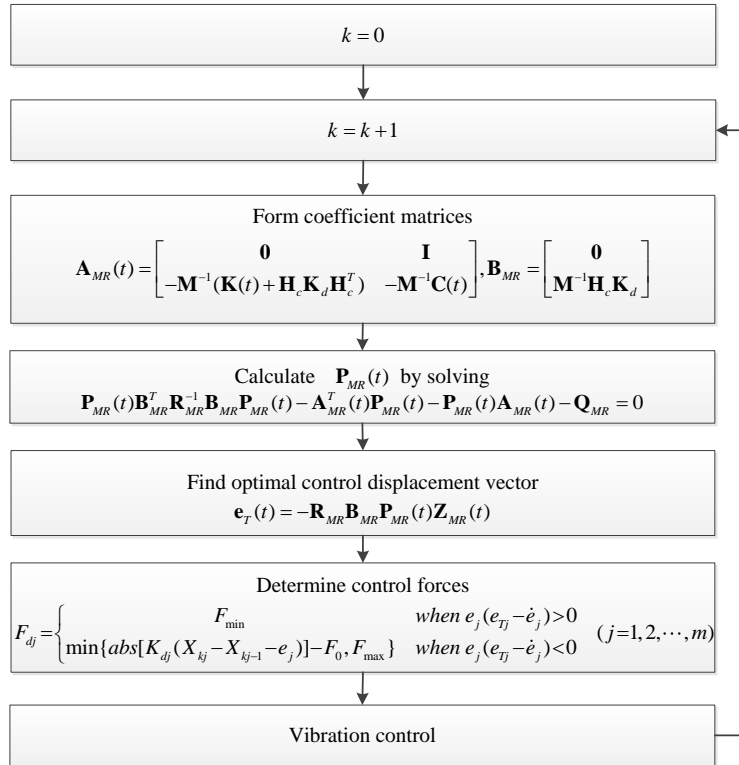


Fig. 3 Flowchart of semi-active control with MR dampers

Step 2: Calculate estimator gain matrix  $\mathbf{K}_k$  using Eq. (15) with the time-varying factor correction matrix determined in Step 1.

Step 3: Generate unknown parametric vector  $\hat{\mathbf{Z}}_k$  using Eq. (7) based on the estimator gain matrix calculated in Step 2 and the current correction term.

Step 4: Update estimation error covariance matrix  $\mathbf{P}_k$  by Eq. (16).

Step 5: Estimate unknown excitation  $\hat{\mathbf{f}}_k$  using Eq. (17) with the unknown parametric vector identified in Step 3.

Step 6: Take the increment  $k = k + 1$ . Form coefficient matrices  $\mathbf{A}_{MR k+1}$  and  $\mathbf{B}_{MR}$  based on Eq. (27) as follows

$$\mathbf{A}_{MR k+1} = \begin{bmatrix} \mathbf{0} & \mathbf{I} \\ -\mathbf{M}^{-1}(\mathbf{K}_{id k} + \mathbf{H}_c \mathbf{K}_d \mathbf{H}_c^T) & -\mathbf{M}^{-1} \mathbf{C}_{id k} \end{bmatrix}, \mathbf{B}_{MR} = \begin{bmatrix} \mathbf{0} \\ \mathbf{M}^{-1} \mathbf{H}_c \mathbf{K}_d \end{bmatrix} \quad (32)$$

where the stiffness matrix  $\mathbf{K}_{id k}$  and damping matrix  $\mathbf{C}_{id k}$  of the building structure are constructed using the stiffness coefficients and damping coefficients identified from the health monitoring

system in Step 3 at time  $t = k\Delta t$ .

Step 7: Calculate the matrix  $\mathbf{P}_{MR k+1}$  by solving the following Riccati equation

$$\mathbf{P}_{MR k+1} \mathbf{B}_{MR}^T \mathbf{R}_{MR}^{-1} \mathbf{B}_{MR} \mathbf{P}_{MR k+1} - \mathbf{A}_{MR k+1}^T \mathbf{P}_{MR k+1} - \mathbf{P}_{MR k+1} \mathbf{A}_{MR k+1} - \mathbf{Q}_{MR} = 0 \tag{33}$$

where the coefficient matrices  $\mathbf{A}_{MR k+1}$  and  $\mathbf{B}_{MR}$  are formed in Step 6.

Step 8: Find optimal control displacement vector  $\mathbf{e}_{T k+1}$  at time  $t = (k + 1)\Delta t$  as

$$\mathbf{e}_{T k+1} = -\mathbf{R}_{MR} \mathbf{B}_{MR} \mathbf{P}_{MR k+1} \mathbf{Z}_{MR k+1} \tag{34}$$

where the matrix  $\mathbf{P}_{MR k+1}$  is calculated in Step 7 and the state vector  $\mathbf{Z}_{MR k+1}$  is composed of structural displacement and velocity responses at time  $t = (k + 1)\Delta t$ .

Step 9: Determine control forces based on the semi-active control strategy as shown in Eq. (31).

Step 10: Calculate measurement vector at time  $t = (k + 1)\Delta t$  for the identification of structural parameter and excitation as well as damage detection based on the measured structural acceleration responses  $\ddot{\mathbf{X}}_{k+1}$  and the measured control forces  $\mathbf{f}_{k+1}^*$

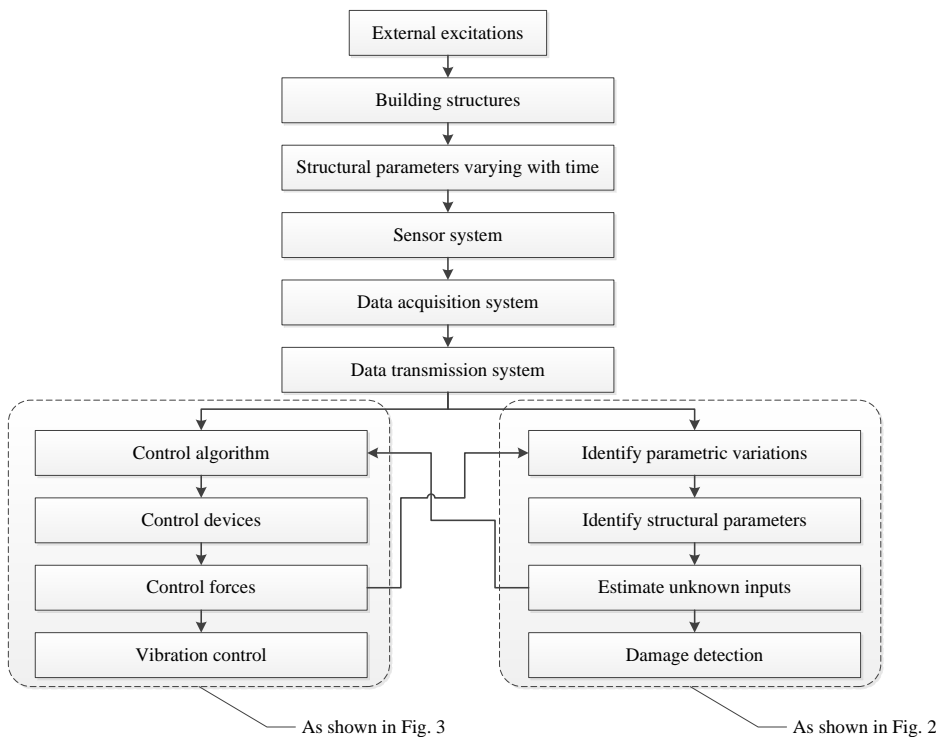


Fig. 4 Flowchart of a real-time integrated procedure for both structural health monitoring and vibration control

$$\mathbf{y}_{k+1} = -\mathbf{M}\ddot{\mathbf{X}}_{k+1} + \boldsymbol{\varphi}^* \mathbf{f}_{k+1}^* \quad (35)$$

where  $\boldsymbol{\varphi}^* = \mathbf{H}_c$ . Return to Step 1 until the discrete time  $t = (k+1)\Delta t$  is the last datum.

A flow chart of the integrated health monitoring and vibration control system for the building structure is shown in Fig. 4. In this integrated system, the health monitoring system and vibration control system are combined together for both system identification and vibration control. The control forces are first measured and transmitted to the health monitoring system in real-time for the identification of structural parameter and excitation as well as damage detection. The time-varying structural parameters and ground excitation, identified from the health monitoring system in real time, are then transmitted to the vibration control system on line to determine optimal control forces to mitigate the structural responses in the next step. The iteration of the above two steps of system identification and vibration control forms the on-line integrated structural health monitoring and vibration control.

## 5. Numerical example

### 5.1 Description of example building structure

A simple five-story shear building is chosen as the example building structure. It has the identical story height of 3 meters (see Fig. 1(a)). The building structure has uniform mass  $m = 5.1 \times 10^3 \text{ kg}$  and uniform horizontal story (shear) stiffness  $k = 1.334 \times 10^7 \text{ N/m}$  for all five stories. The five natural frequencies of the building structures are calculated as 2.317, 6.762, 10.661, 13.695, and 15.620 Hz. The acceleration responses of the building structure are measured by five accelerometers with one on each floor of the building structure. From a practical viewpoint, the white noise of 2% intensity is added to the calculated acceleration response as the measured acceleration response. The noise intensity is defined as the ratio of the root mean square of the noise to the root mean square of the acceleration response. Since the highest natural frequency of the building is 15.620 Hz, a low-pass filter with a cut off frequency of 30 Hz is applied to the noise-polluted acceleration responses. The displacement and velocity responses of the building are obtained from the measured noise-polluted acceleration responses through numerical integrations. On each story of the building, a semi-active MR damper is installed with a chevron brace that connects two neighboring floors. The ratios of the brace horizontal stiffness to the structure horizontal stiffness  $k_d/k$  are selected as one and the same for all the building stories. The properties of the MR dampers are listed in Table 1. Damper forces are measured by five force transducers with one for each MR damper, and the RMS-noise of 1% intensity is added to the calculated control force as the measured control force.

Table 1 Basic parameters of MR damper and fluid

Parameters of MR damper					Parameters of smart material		
$L(\text{m})$	$h(\text{m})$	$b(\text{m})$	$A_p(\text{m}^2)$	$P_y(\text{kN})$	$\eta(\text{k Pa s})$	$\tau_{y \text{ min}}(\text{k Pa})$	$\tau_{y \text{ max}}(\text{k Pa})$
0.5	0.002	0.75	0.04	0.05	0.0002	0.05	10



$\hat{\mathbf{Z}}_0 = [1.25\mathbf{K}_\theta \quad 1 \times 1.25\mathbf{K}_\theta \quad 1]^T$ . The initial estimation error covariance matrix is set as  $\mathbf{P}_0 = 10^7 \times \mathbf{I}_{2n+1}$ , where  $\mathbf{I}_{2n+1}$  represents a  $(2n+1) \times (2n+1)$  identity matrix. For the controlled building structure with semi-active MR dampers subjected to earthquake excitation, the semi-active control forces could be measured by force transducers as the measured excitation  $\mathbf{f}^*(t)$ , while the earthquake ground acceleration  $\ddot{x}_g(t)$  could be treated as the unknown excitation  $\mathbf{f}(t)$ . The influence matrix of the unknown excitations can be set as  $\boldsymbol{\varphi} = \mathbf{H}_e = -\mathbf{M}[1 \quad 1 \quad 1 \quad 1 \quad 1]^T$ . The influence matrix of the known inputs  $\boldsymbol{\varphi}^* = \mathbf{H}_c$  reflects the location of the semi-active MR dampers. The time-varying correction factor matrix is set as  $\boldsymbol{\lambda}_k = \mathbf{I}_m$  during the time period from  $t = 0s$  to  $t = 2s$  in order to obtain the covariance matrix of noise  $\mathbf{R} = 1/(1000-1) \times \sum_{i=1}^{1000} [(\boldsymbol{\Phi}\mathbf{y}_k - \boldsymbol{\Phi}\mathbf{H}_k\hat{\mathbf{Z}}_k)(\boldsymbol{\Phi}\mathbf{y}_k - \boldsymbol{\Phi}\mathbf{H}_k\hat{\mathbf{Z}}_k)^T]$ . The noise covariance matrix calculated is then used for every time step subsequently.

Fig. 5 presents the identified results of time varying stiffness coefficients of the five stories of the building structure. Fig. 6 shows the identified results of two coefficients  $\alpha$  and  $\beta$ . In Figs. 5 and 6, the identified results are presented as dash lines but the real values are presented as solid lines for comparison. The initial values of time-varying story stiffness coefficients at  $t=0$  are taken as 1.25 times the original stiffness coefficients in the calculation. It can be seen that after a very short time period (less than 1.25s), the identified results converge to the actual ones and some spikes appear near  $t=0$ . It can also be seen from Fig. 5 that the proposed algorithm has a very good tracking ability for capturing slightly changed stiffness in a very short time period from 8s to 9s.

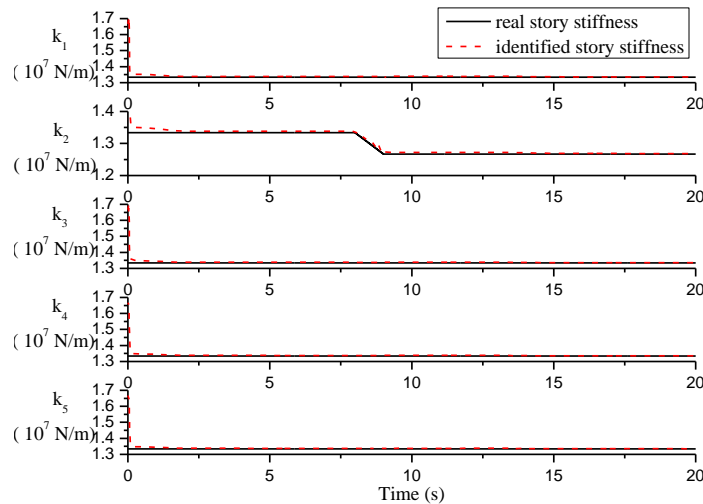


Fig. 5 Identified results of story stiffness

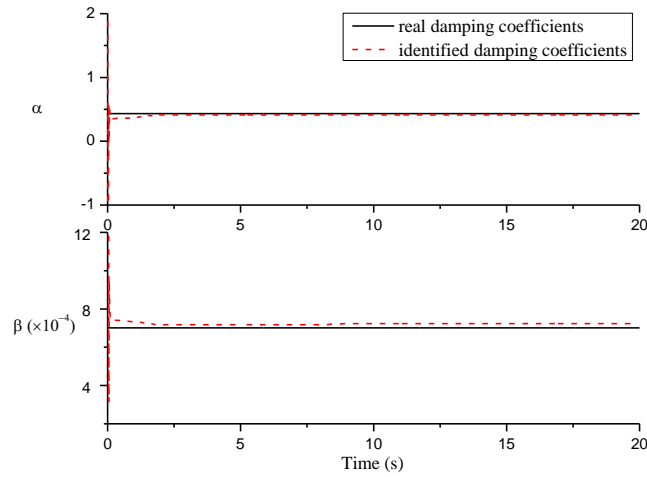


Fig. 6 Identified results of Rayleigh damping coefficients

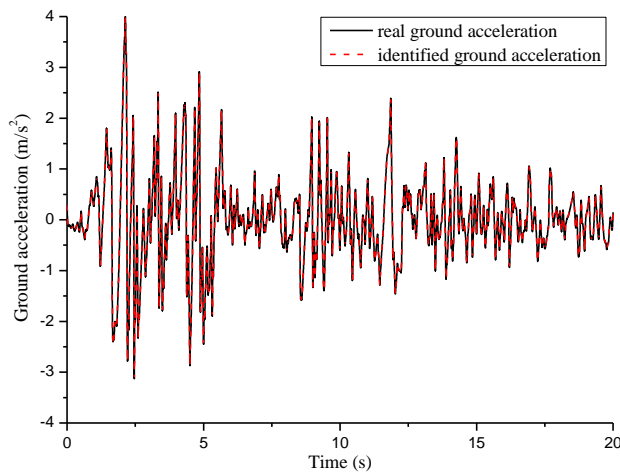


Fig. 7 Identified results of unknown earthquake-induced ground acceleration

The results presented in Fig. 6 also show that the proposed algorithm can identify the two damping coefficients accurately. In summary, the proposed algorithm can identify time-varying structural stiffness and damping coefficients accurately and therefore can detect structural damage precisely on-line. The identified results of the unknown earthquake-induced ground acceleration are presented in Fig. 7 with dash lines and compared with the actual ones with solid lines, and the average identification error of the ground acceleration is only 3.25%. Clearly, the proposed algorithm is capable of identifying the unknown excitation very well.

### 5.3 Performance of semi-active control with MR dampers

To evaluate the semi-active control performance, the seismic record El Centro NS (1940) is selected as input to the example building. The peak ground acceleration of the seismic records is scaled from  $3.417 \text{ m/s}^2$  to  $4.0 \text{ m/s}^2$ . The stiffness matrix and damping matrix of the example building is constructed using the stiffness coefficients and damping coefficients identified from the health monitoring system accordingly. The matrix  $\mathbf{A}_{MR}(t)$  in Eq. (27) and the matrix  $\mathbf{P}_{MR}(t)$  in Eq. (30) are reconstructed at each time step. The ratios of the brace horizontal stiffness to the structure horizontal stiffness of all the five semi-active MR dampers are assigned of the same value of 1. Five accelerometers and five force transducers with one accelerometer and one force transducer for each story are necessary to realize the feedback control. In the numerical investigation of semi-active control performance, the corresponding computed building responses and damper forces are taken as the relevant feedback instead of the signals from the sensors in practice. In the implementation of the clipped optimal displacement control strategy, the two weighting matrices  $\mathbf{Q}_{MR}$  and  $\mathbf{R}_{MR}$  are selected as the unit diagonal matrix multiplied by a factor  $1 \times 10^5$  and  $0.00001$ , respectively, after a trial and error study.

Demonstrated in Fig. 8 are the variations of the peak displacement, velocity, and acceleration responses of the example building without control, with passive-on control, and with semi-active control. The passive-on control is actually a passive control by setting the maximum damping in the MR damper. It can be seen that the peak responses of all the building floors under semi-active control are substantially reduced in comparison with those with passive-on control and without control. Clearly, the semi-active control with the clipped optimal displacement control algorithm can effectively suppress the seismic responses of the building structure.

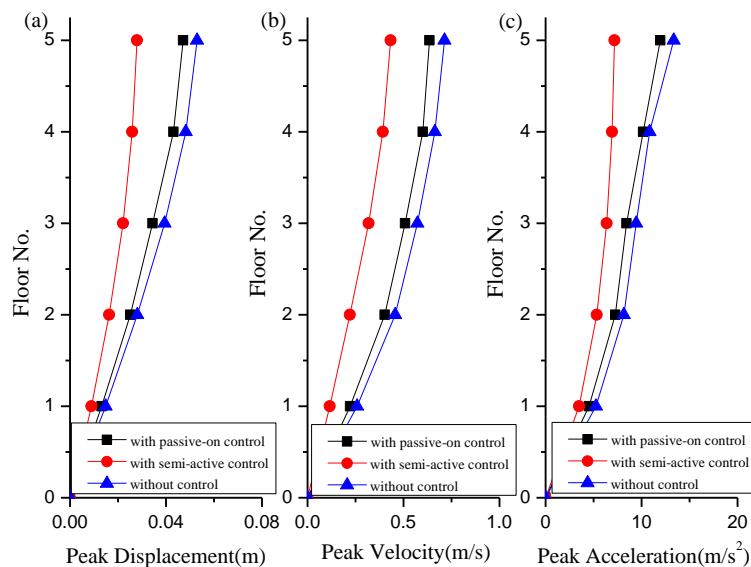


Fig. 8 Comparison of control performance without control and with semi-active control and passive-on control

### 5.4 Comparison

To further demonstrate the necessity and advantage of the proposed integrated procedure, the performance of semi-active control using on-line updated structural parameters is compared with that without updating structural parameters and that with passive-on control. Moreover, the accuracy of the parameter and excitation identification of the building structure with time-varying structural parameters in control algorithm is compared to that with constant structural parameters in control algorithm.

The semi-active control performance is evaluated in terms of two widely-accepted sets of normalized performance indices. The first set of the performance indices is related to the building responses, which include peak- and RMS-based inter-story drift ratios ( $J_1$  and  $J_3$ ) and peak- and RMS-based absolute acceleration responses ( $J_2$  and  $J_4$ ) expressed by

$$J_1 = \frac{\max_{t,i} |dx_i^c(t)|/h_i}{\max_{t,i} |dx_i^n(t)|/h_i} \tag{37}$$

$$J_2 = \frac{\max_{t,i} |\ddot{x}_i^c(t)|}{\max_{t,i} |\ddot{x}_i^n(t)|} \tag{38}$$

$$J_3 = \frac{\max_{t,i} \|dx_i^c(t)\|/h_i}{\max_{t,i} \|dx_i^n(t)\|/h_i} \tag{39}$$

$$J_4 = \frac{\max_{t,i} \|\ddot{x}_i^c(t)\|}{\max_{t,i} \|\ddot{x}_i^n(t)\|} \tag{40}$$

where  $dx_i^c(t)$  and  $dx_i^n(t)$  are the inter-story drifts of the  $i$ th story of the building with and without control, respectively;  $h_i$  is the height of the  $i$ th story;  $|dx_i^c(t)|/h_i$  and  $|dx_i^n(t)|/h_i$  are the inter-story drift ratios of the  $i$ th story of the building with and without control, respectively;  $\ddot{x}_i^c(t)$  and  $\ddot{x}_i^n(t)$  are the absolute acceleration responses of the  $i$ th floor of the building with and without control, respectively. The RMS response quantities within the time duration  $t_f$  under earthquake

excitation are calculated by  $\|\bullet\| = \sqrt{\frac{1}{t_f} \int_0^{t_f} [\bullet]^2 dt}$ . The sign  $\max_{t,i}$  means to find the maximum value

within the given time duration first and among all the building stories afterwards. The second set of performance indices are related to the capacity of control devices. The peak-based control force ( $J_5$ ) is

$$J_5 = \frac{\max_{t,k} |u_k(t)|}{W} \tag{41}$$

Table 2 Performance indices for semi-active vibration control using MR dampers

Index	$J_1$	$J_2$	$J_3$	$J_4$	$J_5$
Passive-on control	0.8703	0.6611	0.8806	0.7532	0.076
Semi-active control without parametric updating	0.8117	0.5744	0.8301	0.6951	0.068
Semi-active control with parametric updating	0.5766	0.5376	0.2439	0.3127	0.054

where  $u_k(t)$  is the control force generated by the  $k$ th control device (MR damper); and  $W$  is the total weight of all the building floors.

Table 2 shows the performance indices of the controlled building with semi-active control (with and without parameter updating) and passive-on control. It can be seen that the proposed semi-active control using MR dampers and considering on-line parameter updating can effectively reduce both the peak and RMS responses of the example building under seismic excitation. The reduction of the RMS responses ( $J_3$  and  $J_4$ ) is even more than that of the peak responses ( $J_1$  and  $J_2$ ). It can also be seen that the semi-active control with on-line parameter updating has much higher control performance than that with passive-on control. The control force index further shows that with passive-on control, the control force required is also more than that using semi-active control with on-line parameter updating. Therefore, the on-line parameter updating is necessary to ensure higher control performance and less control force. The above observation can be further confirmed through the comparison of the time histories of displacement, velocity and acceleration responses of the top floor of the building without control, with passive-on control, and with semi-active control. Fig. 9 shows the time histories of acceleration responses of the top floor of the building for various cases as an example.

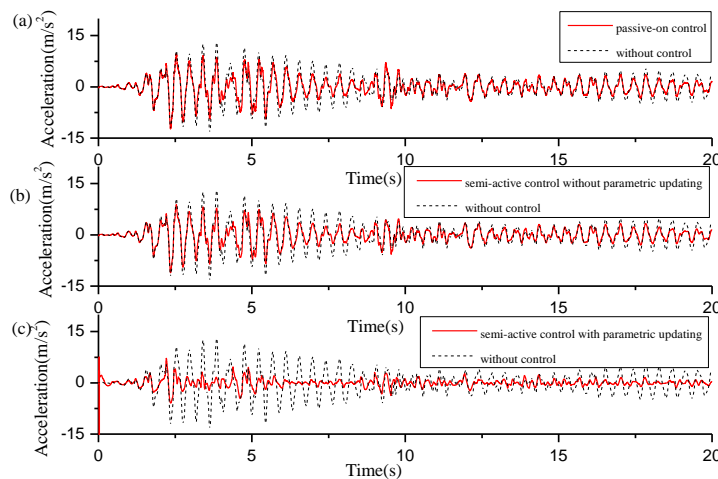


Fig. 9 Comparison of acceleration response time histories of the building structure at the top floor

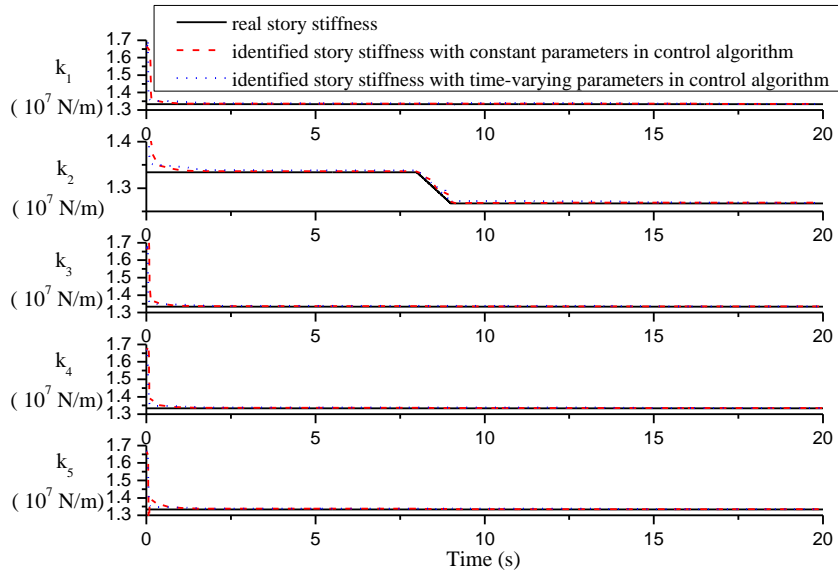


Fig. 10 Comparison of identified results of story stiffness

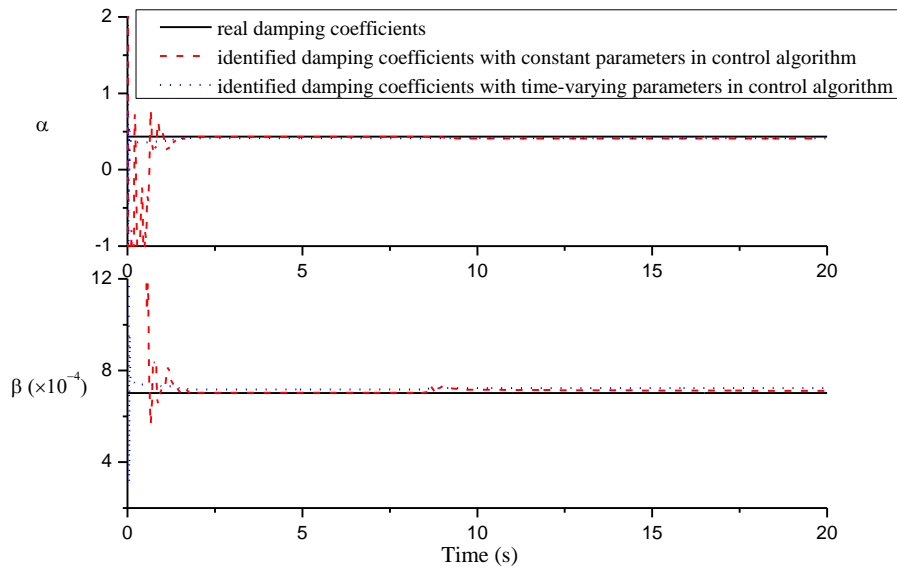


Fig. 11 Comparison of identified results of Rayleigh damping coefficients

Figs. 10 and 11 present the identified results of time-varying stiffness coefficients of the five stories of the controlled building and the two coefficients  $\alpha$  and  $\beta$ , respectively, with and without considering time-varying structural parameters in control algorithm. In Figs. 10 and 11, the identified results for the controlled building without considering time-varying structural parameters in control algorithm are presented as dash lines, whereas those with considering time-varying structural parameters in control algorithm are presented as dot lines and the real values are presented as solid lines for comparison. It can be seen that structural parameter identification of the building with and without considering time-varying structural parameters in control algorithm both have very good tracking ability for capturing time-varying stiffness. Moreover, the identified results of the earthquake-induced ground acceleration are almost the same for the two cases. However, the results presented in Figs. 10 and 11 show that structural parameter identification of the building with considering time-varying structural parameters in control algorithm converges much faster to the real value than that without considering time-varying structural parameter in control algorithm. This is particularly true in the identification of damping coefficients.

## 6. Conclusions

A real-time integrated procedure for both health monitoring and vibration control of a building structure has been presented in this paper so that on one hand, the time-varying structural parameters and unknown excitations of the building structure during earthquake excitation can be identified and, on the other hand, the excessive vibration of the building structure can be effectively mitigated. The time-varying parameter and excitation identifications are based on the least-squares estimation method and the measured structural responses and control forces, whereas the vibration control is fulfilled using semi-active MR dampers, a clipped optimal displacement control algorithm, and on-line identified time varying structural parameters and excitation. The numerical study of an example building shows that the proposed real-time integrated method does effectively suppress the seismic responses of the building compared with the passive-on control and at the same time accurately identify unknown excitations and time-varying structural parameters. The numerical study also manifests that the control performance will deteriorate if only the initial constant structural parameters are taken into account in the semi-active control. However, this does not affect the accuracy of identification of time-varying structural parameters and excitation except for the initial convergent rate.

## Acknowledgements

The authors wish to acknowledge the financial supports from the Research Grants Council of Hong Kong (PolyU 5319/10E). Any opinions and concluding remarks presented in this paper are entirely those of the authors.

## References

Basu, B., Nagarajaiah, S. and Chakraborty, A. (2008), "Online identification of linear time-varying stiffness

- of structural systems by wavelet analysis”, *Struct. Health Monit.*, **7**(1), 21-36.
- Chen, B. and Xu, Y.L. (2008), “Integrated vibration control and health monitoring of building structures using semi-active friction dampers: Part II - Numerical investigation”, *Eng. Struct.*, **30**(3), 573-587.
- Chen, B., Xu, Y.L. and Zhao, X. (2010), “Integrated vibration control and health monitoring of building structures: a time-domain approach”, *Smart Struct. Syst.*, **6**(7), 811-833.
- Deng, F., Rémond, D. and Gaudiller, L. (2011), “Self-adaptive modal control for time-varying structures”, *J. Sound Vib.*, **330**, 3301-15.
- Doebbling, S.W., Farrar, C.R., Prime, M.B. and Shevitz, D.W. (1996), “Damage identification and health monitoring of structural and mechanical systems from changes in their vibration characteristics: a literature review”, Los Alamos National Lab., NM (United States).
- Gattulli, V. and Romeo, F. (2000), “Integrated procedure for identification and control of MDOF structures”, *J. Eng. Mech. - ASCE*, **126**(7), 730-737.
- Gavin, G.P., Hanson, R.D. and Filisko, F.E. (1996), “Electrorheological dampers. Part I: analysis and design”, *J. Appl. Mech. - T ASME*, **63**, 669-675.
- Housner, G.W., Bergman, L.A., Caughey, T.K., Chassiakos, A.G., Claus, R.O., Masri, S.F., Skelton, R.E., Soong, T.T., Spencer, B.F. and Yao, J.T.P. (1997), “Structural control: past present, and future”, *J. Eng. Mech. - ASCE*, **123**, 897-971.
- Huang, Q., Xu, Y.L., Li, J.C., Su, Z.Q. and Liu, H.J. (2012), “Structural damage detection of controlled building structures using frequency response functions”, *J. Sound Vib.*, **331**, 3476-3492.
- Kosmatopoulos, E.B., Smyth, A.W., Masri, S.F. and Chassiakos, A.G. (2001), “Robust adaptive neural estimation of restoring forces in nonlinear structures”, *J. Appl. Mech. - T ASME*, **68**(6), 880-893.
- Lei, Y., Jiang, Y. and Xu, Z. (2012a), “Structural damage detection with limited input and output measurement signals”, *Mech. Syst. Signal Pr.*, **28**, 229-243.
- Lei, Y., Wu, Y. and Li, T. (2012b), “Identification of non-linear structural parameters under limited input and output measurements”, *Int. J. Nonlinear. Mech.*, **47**(10), 1141-1146.
- Mufti, A.A. (2001), *Guidelines for Structural Health Monitoring*, Winnipeg, Manitoba: ISIS Canada.
- Nagarajaiah, S. and Jung, H.J. (2014), “Smart tuned mass dampers: recent developments”, *Smart Struct. Syst.*, **13**(2), 173-176.
- Nishitani, A. and Inoue, Y. (2001), “Overview of the application of active/semiactive control to building structures in Japan”, *Earthq. Eng. Struct. D.*, **30**, 1565-1574.
- Qu, W.L. and Xu, Y.L. (2001), “Semi-active control of seismic response of tall buildings with podium structure using ER/MR dampers”, *Struct. Des. Tall Buil.*, **10**(3), 179-192.
- Ray, L.R. and Tian, L. (1999), “Damage detection in smart structures through sensitivity enhancing feedback control”, *J. Sound Vib.*, **227**(5), 987-1002.
- Sohn, H., Farrar, C.R., Hemez, F.M., Shunk, D.D., Stinemates, D.W. and Nadler, B.R. (2003), *A review of structural health monitoring literature: 1996-2001*, Los Alamos National Laboratory Report, LA-13976-MS.
- Spencer, B.F. and Nagarajaiah, S. (2003), “State of the art of structural control”, *J. Struct. Eng. - ASCE*, **129**(7), 845-56.
- Viscardi, M. and Lecce, L. (2002), “An integrated system for active vibro-acoustic control and damage detection on a typical aeronautical structure”, *Proceedings of the 2002 IEEE International Conference on Control Applications 2002*, Glasgow, Scotland, U.K.
- Wenzel, H. (2009), *Health Monitoring of Bridges*, John Wiley & Sons.
- Xu, Y.L. and Chen, B. (2008), “Integrated vibration control and health monitoring of building structures using semi-active friction dampers: Part I - Theory”, *Eng. Struct.*, **30**(7), 1789-1801.
- Xu, Y.L., Huang, Q., Zhan, S. Su, Z.Q. and Liu, H.J. (2014), “FRF-based structural damage detection of controlled buildings with podium structures: Experimental investigation”, *J. Sound Vib.*, **333**(13), 2762-2775.
- Xu, Y.L., Qu W.L. and Ko J.M. (2000), “Seismic response control of frame structures using magnetorheological/electrorheological dampers”, *Earthq. Eng. Struct. D.*, **29**(5), 557-575.

- Xu, Y.L. and Xia, Y. (2012), *Structural Health Monitoring of Long-span Suspension Bridges*, CRC Press.
- Yang, H.T.Y., Shan, J.Z., Randall, C.J., Hansma, P.K. and Shi, W.X. (2013), "Integration of health monitoring and control of building structures during earthquakes", *J. Eng. Mech. - ASCE*, DOI: 10.1061/(ASCE)EM.1943-7889.0000718.
- Yang, J.N. and Huang, H. (2007), "Sequential non-linear least-square estimation for damage identification of structures with unknown inputs and unknown outputs", *Int. J. Nonlinear. Mech.*, **42**(5), 789-801.
- Yang, J.N., Pan, S. and Lin, S. (2007), "Least-squares estimation with unknown excitations for damage identification of structures", *J. Eng. Mech. - ASCE*, **133**(1), 12-21.